Generalized Mulliken–Hush Analysis of Electronic Coupling Interactions in Compressed π-Stacked Porphyrin–Bridge–Quinone Systems

ARTICLE *in* JOURNAL OF THE AMERICAN CHEMICAL SOCIETY · SEPTEMBER 2005

Impact Factor: 12.11 · DOI: 10.1021/ja050984y · Source: PubMed

4 AUTHORS, INCLUDING:

Youn K. Kang
Sangmyung University
34 PUBLICATIONS **608** CITATIONS

SEE PROFILE

J|A|C|S
ARTICLES
Published on Web 07/21/2005

Generalized Mulliken−Hush Analysis of Electronic Coupling Interactions in Compressed π-Stacked Porphyrin−Bridge−Quinone Systems

Jieru Zheng,[†] Youn K. Kang,[‡] Michael J. Therien,[‡] and David N. Beratan*,[†]

Contribution from the Departments of Chemistry and Biochemistry, Duke University, Durham, North Carolina 27708, and Department of Chemistry, University of Pennsylvania, Philadelphia, Pennsylvania 19104-6323

Received February 15, 2005; E-mail: david.beratan@duke.edu

Abstract: Donor−acceptor interactions were investigated in a series of unusually rigid, cofacially compressed π-stacked porphyrin−bridge−quinone systems. The two-state generalized Mulliken−Hush (GMH) approach was used to compute the coupling matrix elements. The theoretical coupling values evaluated with the GMH method were obtained from configuration interaction calculations using the INDO/S method. The results of this analysis are consistent with the comparatively soft distance dependences observed for both the charge separation and charge recombination reactions. Theoretical studies of model structures indicate that the phenyl units dominate the mediation of the donor−acceptor coupling and that the relatively weak exponential decay of rate with distance arises from the compression of this π-electron stack.

1. Introduction

Electron transfer (ET) plays a crucial role in biology, chemistry, and electronics. Understanding the molecular mechanism of ET is essential for understanding biological function and designing synthetic energy transducing systems.[1−8] DNA-based electron-transfer systems are the subject of particular interest.[7−22,48] In DNA, the average nucleobase−nucleobase interplanar separation is about 3.5 Å, and experimental studies of the distance-dependent kinetics has produced a wide range of results. In contrast to the rapidly expanding information on double-helical DNA-mediated ET reactions, few purely synthetic π-stacked structures exist in which ET kinetics have been measured.

The synthesis of a new series of unusually rigid, π-stacked, compressed porphyrin−bridge−quinone systems ((1−3)a-Zn) that features cofacial aromatic units between electron donor (D) and acceptor (A) units was reported recently.[23] These species differ in many respects from other classes of donor−spacer−acceptor (D−Sp−A) systems. In these systems, a 1,8-naphthyl pillaring motif imposes sub van der Waals interplanar separation (about 3 Å between the closest C atoms) between juxtaposed porphyryl, aromatic bridge, and quinonyl components of the D−Sp−A compounds. The structural compactness also limits the range of distance fluctuations and lateral motion in the D, Sp, and A units in the π-stacked array.[24] The ET kinetics for a family of these rigid π-stacked D−Sp−A systems was reported

[†] Duke University.
[‡] University of Pennsylvania.

(1) *Electron Transfer in Chemistry*; Balzani, V., Piotrowiak, P., Rodgers, M. A. J., Mattay, J., Astruc, D., Gray, H. B., Fukuzumi, S., Mallouk, T. E., Haas, Y., de Silva, A. P., Gould, I. R., Eds.; Wiley-VCH: Weinheim, Germany, 2001; I−V.
(2) *Molecular Electronics: Science and Technology*; Jortner, J., Ratner, M., Eds.; Blackwell Press: Oxford, U.K., 1997.
(3) May, V.; Kühn, O. *Charge and Energy Transfer Dynamics in Molecular Systems*; Wiley-VCH: Berlin, 2000.
(4) *Electron Transfer-From Isolated Molecules to Biomolecules*; Jortner, J., Bixon, M., Eds.; Advances in Chemical Physics Series 106-107; Wiley: New York, 1999.
(5) Gray, H. B.; Winkler, J. R. *Q. Rev. Biophys.* **2003**, *36*, 341.
(6) *Bioelectronics*; Willner, E., Katz, E., Eds.; Wiley-VCH: Weinheim, Germany, 2005.
(7) *Long-Range Charge Transfer in DNA (I and II)*; Schuster, G. B., Ed.; Topics in Current Chemistry Series; Springer-Verlag: Berlin, New York, 2004; Vols. 236 and 237.
(8) Endres, R. G.; Cox, D. L.; Singh, R. R. P. *Rev. Mod. Phys.* **2004**, *76*, 195.
(9) Purugganan, M. D.; Kumar, C. V.; Turro, N. J.; Barton, J. K. *Science* **1988**, *241*, 1645.
(10) Murphy, C. J.; Arkin, M. R.; Jenkins, Y.; Ghatlia, N. D.; Bossmann, S. H.; Turro, N. J.; Barton, J. K. *Science* **1993**, *262*, 1025.
(11) Arkin, M. R.; Stemp, E. D. A.; Holmlin, R. E.; Barton, J. K.; Hörmann, A.; Olson, E. J. C.; Barbara, P. F. *Science* **1996**, *273*, 475.
(12) Kelley, S. O.; Jackson, N. M.; Hill, M. G.; Barton, J. K. *Angew. Chem., Int. Ed.* **1999**, *38*, 941.
(13) Wan, C. Z.; Fiebig, T.; Kelley, S. O.; Treadway, C. R.; Barton, J. K.; Zewail, A. H. *Proc. Natl. Acad. Sci. U.S.A.* **1999**, *96*, 6014.
(14) Lewis, F. D.; Wu, T.; Zhang, Y.; Letsinger, R. L.; Greenfield, S. R.; Wasielewski, M. R. *Science* **1997**, *277*, 673.
(15) Lewis, F. D.; Liu, X.; Miller, S. E.; Wasielewski, M. R. *J. Am. Chem. Soc.* **1999**, *121*, 9746.
(16) Lewis, F. D.; Liu, X.; Liu, J.; Miller, S. E.; Hayes, R. T.; Wasielewski, M. R. *Nature* **2000**, *406*, 51.
(17) Lewis, F. D.; Wu, T.; Liu, X.; Letsinger, R. L.; Greenfield, S. R.; Miller, S. E.; Wasielewski, M. R. *J. Am. Chem. Soc.* **2000**, *122*, 2889.
(18) Lewis, F. D.; Kalgutkar, R. S.; Wu, Y.; Liu, X.; Liu, J.; Hayes, R. T.; Miller, S. E.; Wasielewski, M. R. *J. Am. Chem. Soc.* **2000**, *122*, 12346.
(19) Meade, T. J.; Kayyem, J. F. *Angew. Chem., Int. Ed. Engl.* **1995**, *34*, 352.
(20) Meggers, E.; Kusch, D.; Spichty, M.; Wille, U.; Giese, B. *Angew. Chem., Int. Ed.* **1998**, *37*, 460.
(21) Meggers, E.; Michel-Beyerle, M. E.; Giese, B. *J. Am. Chem. Soc.* **1998**, *120*, 12950.
(22) Fukui, K.; Tanaka, K. *Angew. Chem., Int. Ed.* **1998**, *37*, 158.
(23) Iovine, P. M.; Kellett, M. A.; Redmore, N. P.; Therien, M. J. *J. Am. Chem. Soc.* **2000**, *122*, 8717.
(24) Iovine, P. M.; Veglia, G.; Furst, G.; Therien, M. J. *J. Am. Chem. Soc.* **2001**, *123*, 5668.

recently.[25] Soft distance dependence of the ET rate (β^r value of $\sim$0.4 Å^{-1}, where β^r is the average exponential decay factor governing distance dependence) for both the charge separation (CS) and the charge recombination (CR) reactions was observed. The aim of this article is to understand the structural origins of this soft distance dependence.

Many groups have developed theoretical methods to describe the mechanisms of electron transfer and to calculate electronic-coupling interactions.[2,26−31] Electron-transfer involving excited states, however, continues to present a considerable challenge to theoretical chemists. Indeed, the accurate description of charge-transfer excited states represents an open challenge to modern theory.[32] The current state of the art makes both geometry optimization and electronic coupling calculations particularly challenging for the excited states. Recently, Newton and Cave introduced a generalized Mulliken−Hush (GMH) approach[33,34,40] to compute donor−acceptor interactions, based on the pioneering models of Mulliken[35] and Hush.[36−38] This approach can be used to calculate H_{DA} for both ground- and excited-state electron-transfer reactions.[39]

In this article, we use the two-state generalized Mulliken−Hush approach with INDO wave functions to calculate H_{DA} for both the CS and CR reactions in these π-stacked porphyrin−bridge−quinone structures.

2. Theoretical Method

The two-state generalized Mulliken−Hush approximation computes H_{DA} as:[33,34,39,40]

$$H_{DA} = \frac{\mu_{12}\Delta E_{12}}{\Delta\mu_{12}^{D}} = \frac{\mu_{12}\Delta E_{12}}{(\Delta\mu_{12}{}^{2} + 4\mu_{12}{}^{2})^{1/2}} \quad (1)$$

where μ_{12} is the transition dipole moment connecting the two adiabatic states in the charge transition, $\Delta\mu_{12}$ is the difference in adiabatic state dipole moments, $\Delta\mu_{12}^{D}$ is the difference in diabatic state dipole moments, and ΔE_{12} is the energy difference between the initial and final adiabatic states.

For simplicity, we use a three-state model. The three diabatic states are a donor ground state (GS), a donor locally excited state (LE),[41] and a charge-transfer state (CT) with the "transferring electron" localized on the acceptor. The adiabatic states are assumed to be composed of these three diabatic states. For weak donor−acceptor interactions, the adiabatic states are nearly equivalent to the diabatic states.[39]

In the coupling calculation, the three states (GS, LE, and CT) are treated in a pairwise fashion. For the charge separation process, the LE and CT states are described with a two-state GMH model; for charge recombination, the CT and GS states are used. Electronic coupling is obtained from configuration interaction (CI) calculations using the INDO/S method of Zerner and co-workers.[42] Previous studies have shown that the INDO/S yields reliable values of H_{DA} for a variety of electron-transfer processes involving organic compounds and metal-containing species.[43−47] As was described previously,[45] we evaluate H_{DA} directly from the charge-localized diabatic states obtained from self-consistent-field (SCF) and CI/S calculations.

3. Results and Discussion

3.1. Structures. We used two methods to build optimized structures for the series of porphyrin−bridge−quinone systems. One approach applied to structures (1−3)a-Zn is the semiempirical PM3 method implemented in HyperChem4.5.[51] We also used density functional theory (DFT) (B3LYP with 6-31G* basis set) to optimize structures (1−2)a-Zn in Gaussian98.[52] Figure 1 shows the PM3- and DFT-optimized 2a-Zn structures.

Because of the computational costs, the DFT structure of 3a-Zn was built based on the 2a-Zn DFT geometry. The scheme for building 3a-Zn is to maximize the structural overlap of the phenyl rings (above the porphyrin) between 2a-Zn and the phenyl-naphthyl-quinonyl building block (see Figure S1 in the Supporting Information).

Comparison of the experimental structural data (NMR, X-ray) with the PM3- and DFT-optimized geometries (for 2a-Zn) is shown in Tables 1 and 2.[53]

There is a large difference in the H_6-H_{20} distance (see Table 1) between the PM3 and DFT structures, as well as distance F (the sub van der Waals separation between the H_5 nucleus of the naphthyl pillar attached to the intervening phenyl spacer of 2a-Zn and the porphyrin least-squares plane) in Table 2. These distances reflect the interplanar separation of the phenyl and porphyryl rings. In both cases, the distances derived from DFT-based structures reflect a more compressed π-stack and are

(25) Kang, Y. K.; Rubtsov, I. V.; Iovine, P. M.; Chen, J.; Therien, M. J. *J. Am. Chem. Soc.* **2002**, *124*, 8275.
(26) Yaliraki, S. N.; Roitberg, A. E.; Gonzalez, C.; Mujica, V.; Ratner, M. A. *J. Chem. Phys.* **1999**, *111*, 6997.
(27) Brandbyge, M.; Mozos, J.-L.; Ordejon, P.; Taylor, J.; Stokbro, K. *Phys. Rev. B* **2002**, *65*, 165401.
(28) Nitzan, A.; Galperin, M.; Ingold, G. L.; Grabert, H. *J. Chem. Phys.* **2002**, *117*, 10837.
(29) Heath, J. R.; Ratner, M. A. *Phys. Today* **2003**, *56*, 43.
(30) Nitzan, A.; Ratner, M. A. *Science* **2003**, *300*, 1384.
(31) Nitzan, A. *Annu. Rev. Phys. Chem.* **2001**, *52*, 681.
(32) Dreuw, A.; Worth, G. A.; Cederbaum, L. S.; Head-Gordon, M. *J. Phys. Chem.* **2004**, *108*, 19049.
(33) Cave, R. J.; Newton, M. D. *Chem. Phys. Lett.* **1996**, *249*, 15.
(34) Cave, R. J.; Newton, M. D. *J. Chem. Phys.* **1997**, *106*, 9213.
(35) Mulliken, R. S. *J. Am. Chem. Soc.* **1952**, *74*, 1.
(36) Hush, N. S. *Prog. Inorg. Chem.* **1967**, *8*, 391.
(37) Hush, N. S. *Electrochim. Acta* **1968**, *13*, 1005.
(38) Reimers, J. R.; Hush, N. S. *J. Phys. Chem.* **1991**, *95*, 9773.
(39) Rust, M.; Lappe, J.; Cave, R. J. *J. Phys. Chem. A* **2002**, *106*, 3930.
(40) Creutz, C.; Newton, M. D.; Sutin, N. *J. Photochem. Photobiol., A* **1994**, *82*, 47.
(41) There are two LE states for porphyrin structure (polarized X and Y). The reported electronic coupling data in this article were the average result of those two states.
(42) (a) Zerner, M. C.; Loew, G. H.; Kirchner, R. F.; MuellerWesterhoff, U. T. *J. Am. Chem. Soc.* **1980**, *102*, 589. (b) Thompson, M. A. (mark@arguslab.com). *ArgusLab 4.0*; Planaria Software LLC: Seattle, WA, 2004 (http://www.arguslab.com).
(43) Newton, M. D. *J. Phys. Chem.* **1991**, *95*, 30.
(44) Newton, M. D.; Ohta, K.; Zhong, E. *J. Phys. Chem.* **1991**, *95*, 2317.
(45) Newton, M. D. *Chem. Rev.* **1991**, *91*, 767.
(46) Cave, R. J.; Newton, M. D.; Kumar, K.; Zimmt, M. B. *J. Phys. Chem.* **1995**, *99*, 17501.
(47) Ungar, L. W.; Newton, M. D.; Voth, G. A. *J. Phys. Chem. B* **1999**, *103*, 7367.
(48) Lee, M.; Shephard, M. J.; Risser, S. M.; Priyadarshy, S.; Paddon-Row, M. N.; Beratan, D. N. *J. Phys. Chem. A* **2000**, *104*, 7593.
(49) House, H. O.; Koepsell, D. G.; Campbell, W. J. *J. Org. Chem.* **1972**, *37*, 1003.
(50) Clough, R. L.; Kung, W. J.; Marsh, R. E.; Roberts, J. D. *J. Org. Chem.* **1976**, *41*, 3603.
(51) *HyperChem4.5*; Hypercube, Inc.: Gainesville, FL, 1995.
(52) Frisch, M. J.; Trucks, G. W.; Schlegel, H. B.; Scuseria, G. E.; Robb, M. A.; Cheeseman, J. R.; Zakrzewski, V. G.; Montgomery, J. A., Jr.; Stratmann, R. E.; Burant, J. C.; Dapprich, S.; Millam, J. M.; Daniels, A. D.; Kudin, K. N.; Strain, M. C.; Farkas, O.; Tomasi, J.; Barone, V.; Cossi, M.; Cammi, R.; Mennucci, B.; Pomelli, C.; Adamo, C.; Clifford, S.; Ochterski, J.; Petersson, G. A.; Ayala, P. Y.; Cui, Q.; Morokuma, K.; Rega, N.; Salvador, P.; Dannenberg, J. J.; Malick, D. K.; Rabuck, A. D.; Raghavachari, K.; Foresman, J. B.; Cioslowski, J.; Ortiz, J. V.; Baboul, A. G.; Stefanov, B. B.; Liu, G.; Liashenko, A.; Piskorz, P.; Komaromi, I.; Gomperts, R.; Martin, R. L.; Fox, D. J.; Keith, T.; Al-Laham, M. A.; Peng, C. Y.; Nanayakkara, A.; Challacombe, M.; Gill, P. M. W.; Johnson, B.; Chen, W.; Wong, M. W.; Andres, J. L.; Gonzalez, C.; Head-Gordon, M.; Replogle, E. S.; Pople, J. A. *Gaussian 98*, revision A.11.3; Gaussian, Inc.: Pittsburgh, PA, 2002.
(53) The "exptl distance" column in Table 1 is based on the NMR data of molecule **2a** (the same structure as 2a-Zn except without Zn); the "1_{low}" in Tables 1 and 2 is based on the calculated structure using CHARMm, which is published in ref 24; the distance information of 1,8-diphenyl-naphthalene is from X-ray data of refs 49 and 50.

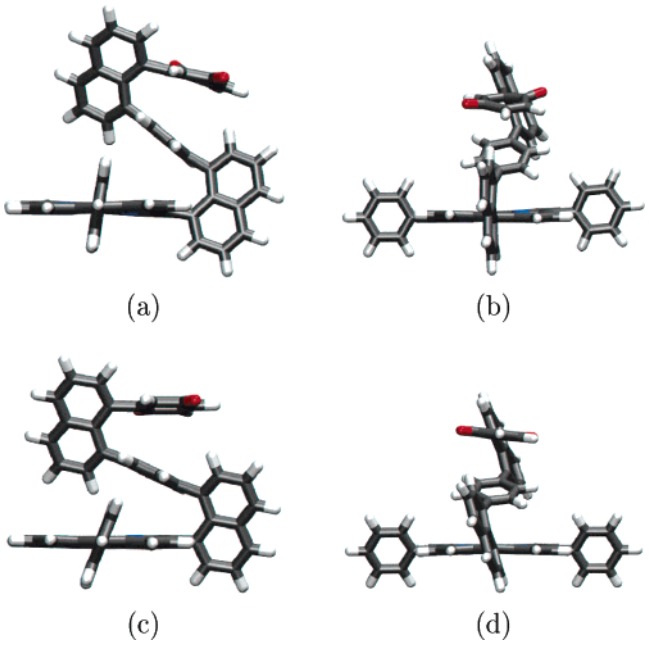

Figure 1. (a) and (b) PM3-based minimum energy structure of 2a-Zn. (a) View along the axis defined by the macrocycle 10 and 20 positions and (b) view along the axis defined by the macrocycle 5 and 15 positions; note that the porphyrin 5 position bears the 1,8-naphthyl pillar. (c) and (d) DFT-based minimum energy structure of 2a-Zn. (c) View along the axis defined by the macrocycle 10 and 20 positions and (d) view along the axis defined by the macrocycle 5 and 15 positions.

Table 1. Comparison between Experimental Interproton Distances with Distances Derived from PM3/DFT Optimized Structures

		calcd distance (Å) for		
atom pair[a]	exptl distance (Å)	1_{low}[b]	2a-Zn(PM3)	2a-Zn(DFT)
H_7-H_8	2.37	2.34	2.39	2.40
H_1-H_{26}	4.00	4.12	4.04	4.32
H_1-H_{28}	2.98	3.21	2.69	2.97
H_2-H_{27}	3.16	3.22	3.30	3.67
H_2-H_{25}	4.87	4.05	4.45	4.17
$H_{16}-H_{17}$	3.09	2.40	2.46	3.30
H_5-H_3	2.93	3.26	2.65	2.84
H_5-H_4	3.28	3.64	4.06	3.97
H_6-H_{20}	3.86	3.32	6.41	4.30
$H_{10}-H_{19}$	3.27	3.31	2.82	2.76
$H_{19}-H_4$	3.06	2.92	3.02	3.26
$H_{16}-H_1$		3.51	3.56	3.94
$H_{16}-H_2$		3.42	3.25	2.84
H_5-NH		2.43		

[a] See Figure S2. [b] 1_{low} is one of 44 calculated structures sharing the lowest CHARMm energy.[24]

Table 2. Distances between π-Stacked Rings

distance label[a]	1,8-diphenyl-naphthalene[b]	1_{low}[b]	2a-Zn(PM3)[b]	2a-Zn(DFT)[b]
A	2.99	2.97	2.99	2.95
B	3.53	3.46	3.62	3.59
C	4.02	3.95	4.18	4.28
D		2.97	3.08	2.99
E		3.35	3.62	3.60
F		2.17	3.64	2.80
G		6.80	6.88	7.11

[a] See Figure S3. [b] In angstroms.

closer to the experimental data. The other clear difference between theoretical predictions is the orientation of the π-stack formed by the phenyl, quinonyl, and porphyryl rings. In the DFT-based structure, the π-stack axis (the line drawn through the center of the phenyl and quinonyl rings) is nearly perpendicular to the porphyryl plane, while in the PM3-based structures, there is a tilt angle of about 70° (see Figure 1a). By comparing the PM3- and DFT-based structures of 2a-Zn, we conclude that the DFT optimization describes the π-stacked geometry more accurately than the PM3 method based on experimentally determined condensed phase structures.[24]

Table 3. Electronic Couplings for (1−3)a-Zn Structures

	PM3 optimized			DFT optimized		
	D–A distance[a] (Å)	CS H_{DA} (eV)	CR H_{DA} (eV)	D–A distance[a] (Å)	CS H_{DA} (eV)	CR H_{DA} (eV)
1a-Zn	3.65	2.27×10^{-1}	2.18×10^{-1}	3.37	3.82×10^{-1}	3.23×10^{-1}
2a-Zn	6.88	4.60×10^{-2}	4.64×10^{-2}	7.11	9.20×10^{-2}	9.25×10^{-2}
3a-Zn	10.54	3.14×10^{-2}	3.14×10^{-2}	10.62	4.11×10^{-2}	4.11×10^{-2}

[a] D−A distance is the porphyrin plane-to-quinonyl centroid distances for computationally determined structures.[55]

3.2. GMH Calculation of Electronic Coupling for (1−3)-a-Zn. Coupling for PM3-Based Structures. Excited-state energies and dipole moments were obtained using the INDO/S SCI method of Zerner et al.[42,54] The state characteristics of the three states (GS, LE, and CT) were deduced from the respective adiabatic dipole moments, charge shifts, and SCI expansion coefficients.

The two-state GMH method was applied to (1−3)a-Zn structures to compute H_{DA}. The calculated coupling values are summarized in Table 3.

We also computed the decay parameter β that describes the distance dependence of the squared electronic coupling. Where the distance is defined as the porphyrin plane-to-quinonyl centroid distance, the computed β for charge separation is 0.59 $Å^{-1}$. It is 0.58 $Å^{-1}$ for the charge recombination process (see Figure 2). The 1a-Zn molecule has a strong electronic coupling (~0.23 eV) for both CS and CR. This likely places the 1a-Zn ET mechanism in the adiabatic regime. Excluding 1a-Zn from the analysis of the distance dependence, β (for structures (2−3)a-Zn) is 0.21 $Å^{-1}$ for both the charge separation process and the charge recombination process. The squared electronic coupling decay for both charge separation and charge recombination is a weak function of distance in these structures, in agreement with the experimental data.[25]

Coupling for DFT-Based Structures. The couplings calculated from DFT-based structures are summarized in Table 3. The distance-dependent H_{DA}^2 decay exponent for both CS and CR processes is $\beta = 0.46$ $Å^{-1}$ based on the 2a-Zn and 3a-Zn analysis. As above, there is a soft distance dependence computed for the squared coupling (see Figure 3) based on these structures.

Comparison of PM3- and DFT-Based Structures. From the structural perspective, the DFT optimization describes the π-stacked geometry more accurately than the PM3 method (the porphyryl−phenyl interplanar separation and phenyl and quinonyl tilt angles with respect to the porphyryl are closer to experiment in DFT-based structures). Table 3 shows that the computed

(54) For 1a-Zn, we included all single excitations from the highest 26 occupied molecular orbitals (MOs) to the lowest 26 virtual MOs; for 2a-Zn we included all single excitations from the highest 34 occupied MOs to the lowest 34 virtual MOs; for 3a-Zn we included all single excitations from the highest 42 occupied MOs to the lowest 42 virtual MOs, and for 4a-Zn we included all single excitations from the highest 50 occupied MOs to the lowest 50 virtual MOs. The number was chosen based on analysis of the convergence of the electronic coupling. These excitations include CI excitations of bridge (π) to bridge (π^*) and donor (π) to bridge (π^*), as well as the porphyrin and quinone local excitations.

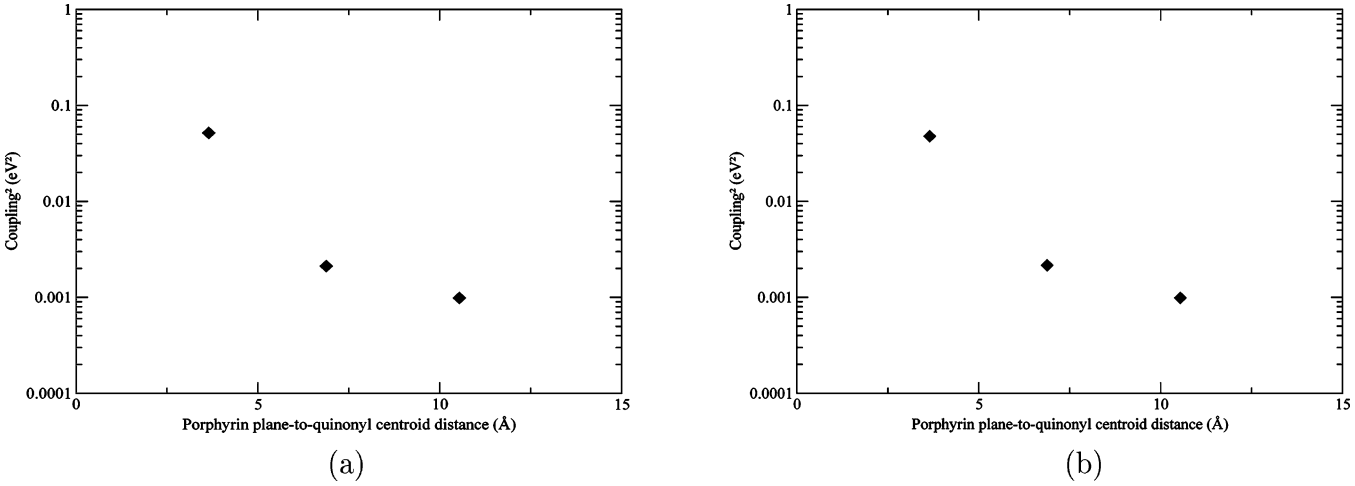

Figure 2. Computed H_{DA}^2 for CS (a) and CR (b) based on PM3-optimized (1−3)a-Zn geometries as a function of porphyrin plane-to-quinonyl centroid distance.

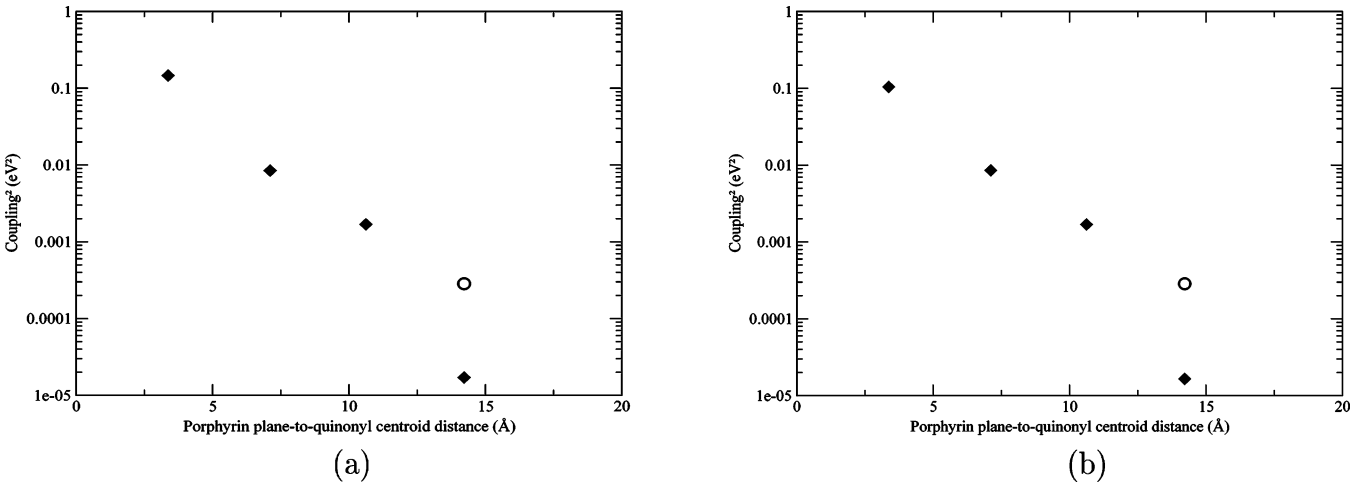

Figure 3. Computed H_{DA}^2 for CS (a) and CR (b) based on DFT-optimized (1−4)a-Zn geometries as a function of porphyrin plane-to-quinonyl centroid distance. (◆) Electronic couplings evaluated for the DFT-based minimum energy (1−4)a-Zn structure. (○) The 4a-Zn′ structure, which corresponds to a modified structure of 4a-Zn with the naphthyl pillars deleted and the middle phenyl ring moved back into the stack (see Figure 8e).

couplings for DFT-based (1−3)a-Zn structures are larger than those of the PM3-based structures (by a factor of 1.3−2.0). The geometry (as well as the somewhat larger couplings) suggests that the DFT-optimized geometries likely describe the π-stack more accurately than the PM3-based structures.

Coupling Calculations for Partial Structures. To understand the influence of the bridge on the electron tunneling interactions and the structural origins of the soft distance dependence of the squared electronic coupling, we calculated H_{DA} for partial structures based on both PM3- and DFT-optimized (2−3)a-Zn geometries. Figures 4 and 5 show the partial structures that were examined (the deleted part is replaced with an H atom). Tables 4 and 5 show the computed couplings.

The detailed calculations on 2a-Zn and 3a-Zn indicate that the phenyl rings between donor and acceptor dominate the coupling mediation. For 2a-Zn, the coupling drops by a factor of 35 to 50 when the phenyl ring is removed (structure 2a-Zn-1; see Figure 4). However, removing either one of the two naphthyl rings decreases the coupling only by about a factor of 2 (structures 2a-Zn-2 and 2a-Zn-3; see Figure 4). A similar trend was found in 3a-Zn. Removing the phenyl ring adjacent to the quinonyl ring (structure 3a-Zn-1; see Figure 5) decreases the coupling by a factor of 35 to 55. Removing the phenyl ring adjacent to the porphyryl ring decreases the coupling by a factor of 70−90 (structure 3a-Zn-2; see Figure 5). However, when one of the naphthyl rings is removed, the coupling only changes by a factor of 1.5 (structures 3a-Zn-3, 3a-Zn-4, and 3a-Zn-5; see Figure 5). The large variation in coupling upon removing a phenyl bridge unit suggests that the π-stack, rather than the "pillars", dominates the electronic propagation through the bridge.

In the structures with both naphthyl pillars removed, we find that the DFT-based coupling is larger than the PM3-based coupling by a factor of 40. A similar trend (a factor of 10) is seen in 3a-Zn-6. However, the calculated DFT-based couplings for the full structures (both 2a-Zn and 3a-Zn) only vary by about a factor of 1.5 from the PM3-based values. Based on the more realistic DFT π-stack, the difference suggests that if π-electron ring stacking is somewhat disrupted (as in the PM3-based 2a-Zn-4 and 3a-Zn-6 structures), the naphthyl bridges make a larger contribution to the overall D−A coupling. Therefore, when we delete the naphthyl bridges in structures with somewhat disrupted π-stacking, the coupling drops dramatically.

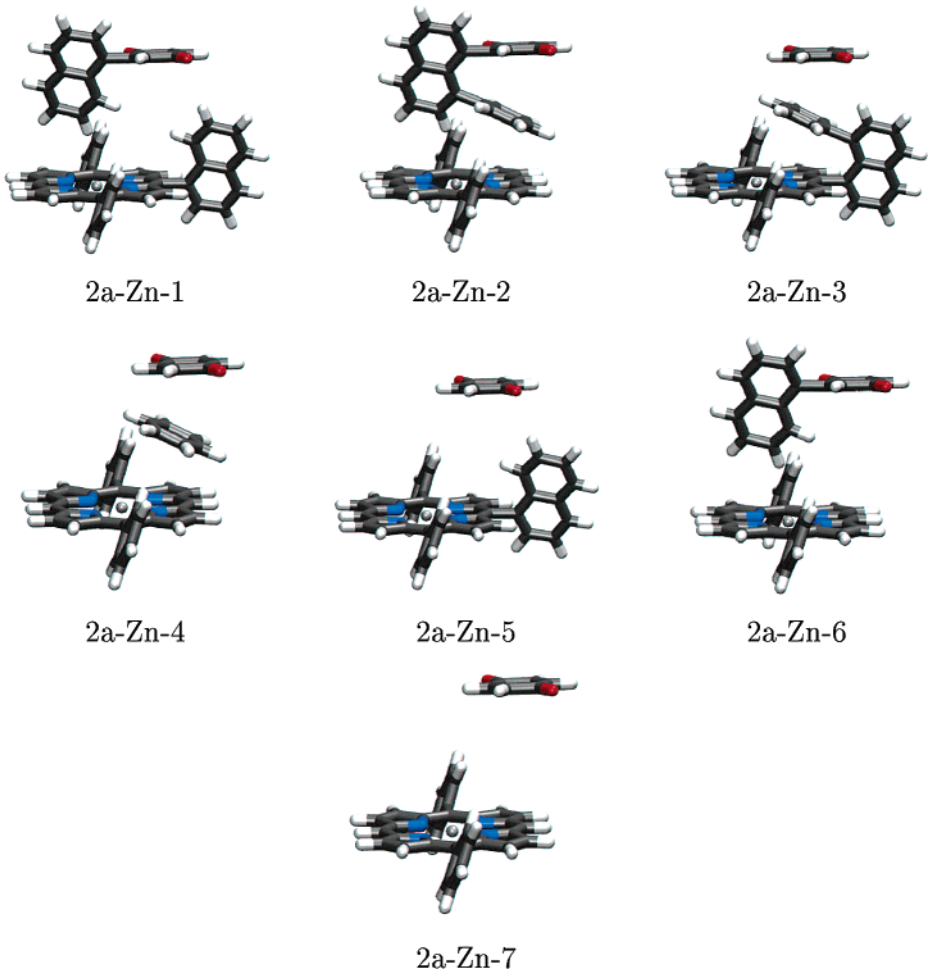

Figure 4. Partial structures used to analyze electronic coupling in 2a-Zn.

Influence of Expanded Interplanar Separation Distances. Both the experimental analysis and our coupling calculations on this series of π-stacked systems suggest that the small β value likely arises from the compression of the π-stack.[25] The overlap of corresponding p_z orbitals in two phenyl rings in approximately D_{6h} geometry changes by about a factor of 3 as the distance between rings changes from 3.0 to 3.5 Å. A simple calculation demonstrates the magnitude of the "compression" effect in the molecules. The closest atom−atom contact, that is, the internuclear distance separating the C1 and C1′ carbon atoms (labeled A and D in Figure S3, part b), is about 3.0 Å (below standard van der Waals separation distances). We expanded the closest contact distance in structures 2a-Zn-4 and 3a-Zn-9 to about 3.5 Å along the axis through the donor and acceptor ring centers (2a-Zn-4′ and 3a-Zn-9′; see Figure 6) and recalculated the couplings (see Table 6). The β value increases to 1.14 $Å^{-1}$ in the expanded structures (2a-Zn-4′ and 3a-Zn-9′), compared with the original β value of 0.13 $Å^{-1}$ for 2a-Zn-4 and 3a-Zn-9. A similiar model calculation that examines the effect upon electronic coupling of changing the angles between the phenyl, quinonyl, and porphyrin planes (rotation while fixing the center position of each ring) such that the rings are nearly parallel to each other (2a-Zn-4″ and 3a-Zn-9″) is shown in Figure 7. Because the distance between the neighboring rings is about 3.5 Å after placing the rings in parallel planes, the effect of this rotation is the same as expanding the closest contact distance between rings from 3.0 to 3.5 Å. The β value we find for parallel ring planes is 1.08 $Å^{-1}$ (see Table 7 for coupling values), which is close to the value of 1.14 $Å^{-1}$ found in previous model calculation with expanded tilted rings. As such, expanding the ring system to van der Waals distances produces *a 1 order of magnitude π-stack compression effect on β*.

3.3. Analysis of 4a-Zn. Using the strategy of Figure S1 (maximizing the structural overlap of the phenyl rings above the porphyryl ring between 2a-Zn and the extended phenyl−naphthyl−quinonyl building block), we constructed an approximate DFT-based 4a-Zn structure, which has not yet been synthesized. The computed charge separation ET coupling is 4.13×10^{-3} eV, and the charge recombination coupling is 4.06×10^{-3} eV. It is clear that the coupling data for 4a-Zn does not fall on a single-exponential line based on the 2a-Zn and 3a-Zn structures (see Figure 3). Closer inspection of the 3a-Zn and 4a-Zn structures (see Figure 8) shows that the position of the middle phenyl ring in 4a-Zn is not aligned (its ring center) with the ring stack in the approximate 4a-Zn structure.

We hypothesized that this decreases the electronic coupling in 4a-Zn compared with an aligned π-stack. To test the stacking-dependent coupling hypothesis, we deleted the naphthyl bridges and moved the middle phenyl ring into alignment with the stack (structure 4a-Zn′; see Figure 8e). The ET coupling increases nearly 1 order of magnitude to 1.69×10^{-2} eV for both CS and CR processes. The squared electronic couplings for (2−3)a-Zn and 4a-Zn′ fit the decay line defined by the short-distance

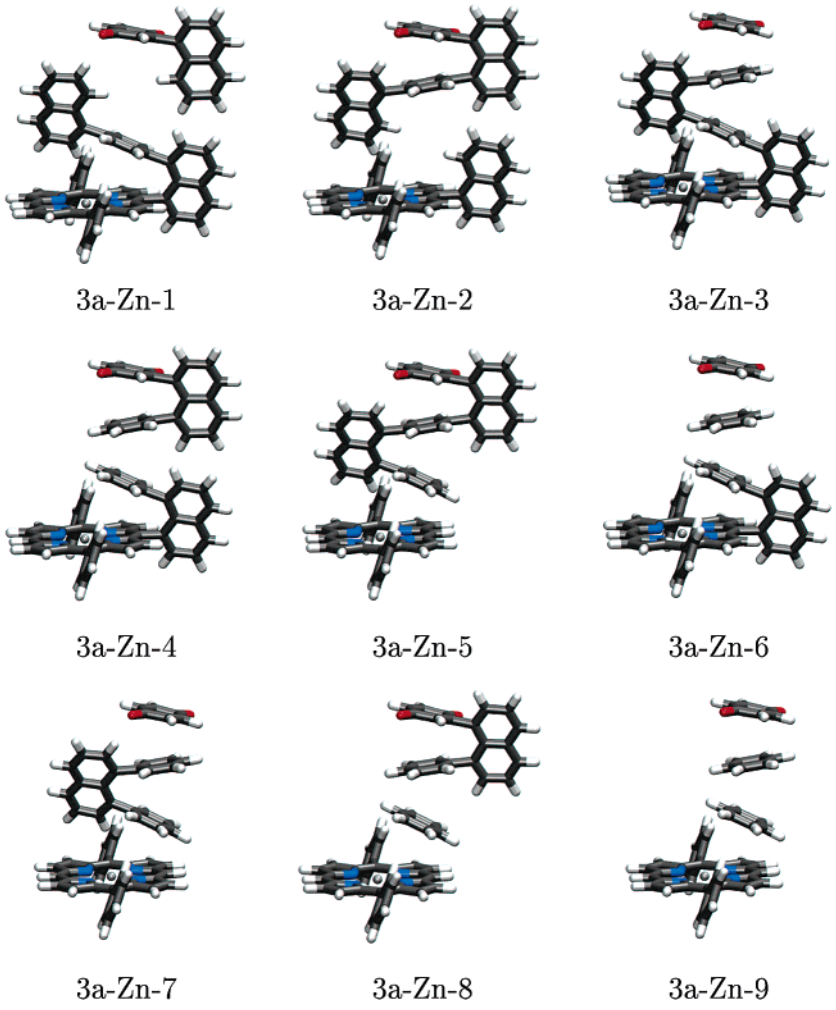

Figure 5. Partial structures used to analyze electronic coupling in 3a-Zn.

Table 4. H_{DA}(eV) for Partial 2a-Zn Structures

	PM3 optimized		DFT optimized	
	CS	CR	CS	CR
2a-Zn-1	1.32×10^{-3}	1.32×10^{-3}	1.58×10^{-3}	1.58×10^{-3}
2a-Zn-2	3.12×10^{-2}	3.13×10^{-2}	4.04×10^{-2}	4.07×10^{-2}
2a-Zn-3	2.10×10^{-2}	2.11×10^{-2}	5.78×10^{-2}	5.82×10^{-2}
2a-Zn-4	1.21×10^{-3}	1.21×10^{-3}	4.21×10^{-2}	4.23×10^{-2}
2a-Zn-5	9.89×10^{-4}	9.91×10^{-4}	1.07×10^{-3}	1.08×10^{-3}
2a-Zn-6	1.50×10^{-4}	1.50×10^{-4}	1.11×10^{-4}	1.11×10^{-4}
2a-Zn-7	1.44×10^{-5}	1.44×10^{-5}	2.33×10^{-5}	2.33×10^{-5}

Table 5. H_{DA}(eV) for Partial 3a-Zn Structures

	PM3 optimized		DFT optimized	
	CS	CR	CS	CR
3a-Zn-1	9.16×10^{-4}	9.19×10^{-4}	7.42×10^{-4}	7.61×10^{-4}
3a-Zn-2	4.62×10^{-4}	4.60×10^{-4}	4.73×10^{-4}	4.83×10^{-4}
3a-Zn-3	2.13×10^{-2}	2.13×10^{-2}	3.40×10^{-2}	3.41×10^{-2}
3a-Zn-4	1.66×10^{-2}	1.66×10^{-2}	3.44×10^{-2}	3.44×10^{-2}
3a-Zn-5	1.48×10^{-2}	1.48×10^{-2}	2.72×10^{-2}	2.73×10^{-2}
3a-Zn-6	3.02×10^{-3}	2.97×10^{-3}	3.13×10^{-2}	3.14×10^{-2}
3a-Zn-7	1.48×10^{-2}	1.48×10^{-2}	2.99×10^{-2}	3.00×10^{-2}
3a-Zn-8	1.18×10^{-2}	1.18×10^{-2}	3.00×10^{-2}	3.02×10^{-2}
3a-Zn-9	7.87×10^{-3}	7.88×10^{-3}	3.35×10^{-2}	3.36×10^{-2}

points after this ring shift (see Figure 3). Therefore, the inconsistency of the coupling for 4a-Zn in its initially modeled geometry with the β value suggested by (2−3)a-Zn likely arises from the sliding of the phenyl ring in the π-stack out of register. We show that displacements of the stacking of this magnitude will cause a considerable decrease in the ET rate. While this model for 4a-Zn may not be reliable, it does show the strong dependence of the coupling on the π-stack structure.

3.4. Analysis of ET Rate Data. The experimental data indicate a soft exponential decay of the ET rates with distance,[25] which is characterized by β^r, where $k_{ET} \propto \exp[-\beta^r R_{DA}]$. Our theoretical analysis only focuses on the distance dependence of the ET coupling. It is important to note that the rate decay parameter (β^r) and the $|H_{DA}|^2$ decay parameter (β) are different because β^r includes any distance dependence of $\Delta G°$ and λ (reorganization energy), in addition to the distance dependence of the coupling.

Several groups have explored the dependence of λ[56−62] in π-stacks. Continuum electrostatics calculations of the outer sphere reorganization energy (λ_o) predict a rapid increase of λ_o with distance at short donor−acceptor distances and a leveling off at longer distances. Indeed, a strong dependence of λ_o on distance is predicted for the molecules studied here based on continuum solvation models. If we use the calculated H_{DA} (this work) and λ_o values with $\Delta G°$ (from experiment) in the nonadiabatic ET rate equation, we can compute a theoretical decay parameter β^r. The value of β^r obtained from a nonadiabatic rate expression with the Marcus (classical) nuclear factor is greater than 1 Å^{-1} when the strongly distance-dependent λ_o

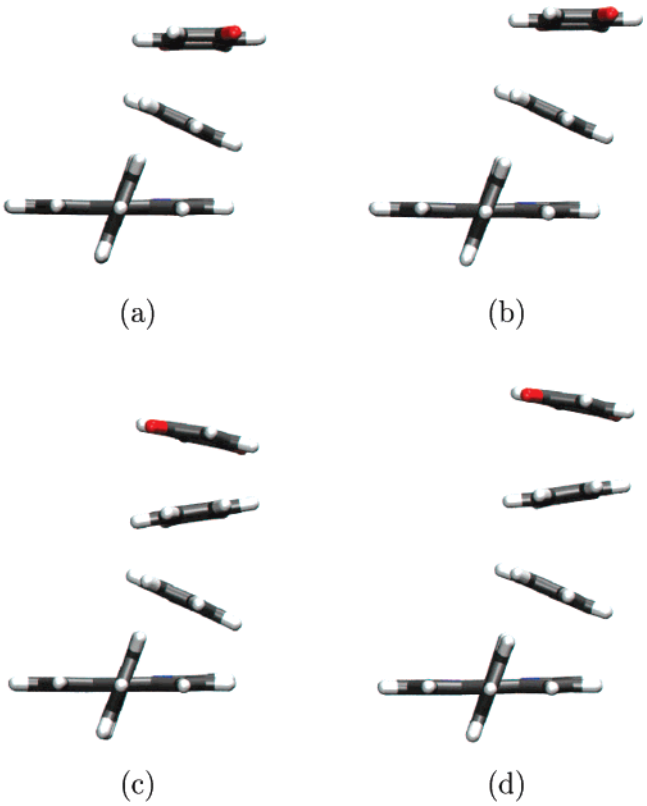

Figure 6. Comparison of partial structures (a) 2a-Zn-4, (b) 2a-Zn-4′, (c) 3a-Zn-9, and (d) 3a-Zn-9′ based on DFT-optimized (2−3)a-Zn geometries. The structures with single prime (b and d) are based on structures (a) and (c) with the closest atom−atom contacts expanded from 3.0 to 3.5 Å along the axis through the centers of the donor and acceptor.

Table 6. H_{DA} (eV) for 2a-Zn-4′ and 3a-Zn-9′ Structures

	D–A distance (Å)	CS	CR
2a-Zn-4′	8.02	9.79×10^{-3}	9.79×10^{-3}
3a-Zn-9′	12.20	9.02×10^{-4}	9.02×10^{-4}

Table 7. H_{DA} (eV) for 2a-Zn-4″ and 3a-Zn-9″ Structures

	D–A distance (Å)	CS	CR
2a-Zn-4″	7.11	3.58×10^{-2}	3.59×10^{-2}
3a-Zn-9″	10.62	5.42×10^{-3}	5.43×10^{-3}

values are used. This is inconsistent with the experimental data (~0.4 $Å^{-1}$). It is important to point out the possiblility that these continuum dielectric computations overestimate the distance dependence of λ_o as pointed out earlier.[56,58] Possible sources of error include delocalization of the donor or acceptor states onto the bridge or anomalously larger electronic polarizability for the π-stacked system. Indeed, a consistent theoretical analysis of observed DNA ET kinetics requires distance-independent reorganization energies.[58] If we also make this assumption for the π-stacks under study here, we conclude that the soft distance dependence of the squared electronic coupling (β) that we calculated accounts for the soft distance dependence of the observed ET rate (β^r).[25] As such, the small β^r value observed is interpreted as originating from compression of the π-stack. The present studies analyze a single geometry for each structure. While thermal fluctuations from the minimal energy geometry of (1−3)a-Zn are expected to be small, computations of H_{DA}^2 should in general be averaged over rapid structural fluctuations when computing the ET rates.[57,63]

Bridge energetics can play an important role in controlling electronic coupling and ET rates.[64] We have found here that β and H_{DA} for CS and CR processes are nearly the same, which is consistent with the fact that porphyrin, porphyrin-excited state, and quinone electron-transfer active orbitals are far in energy from the HOMO/LUMO of the phenyl bridge (about 2.5 eV away). Even adding electron-withdrawing group (−F) or electron-donating group ($-NH_2$) to the phenyl bridge, which shift the HOMO by 0.5−1.0 eV, does not cause H_{DA}(CS) andH_{DA}(CR) values to differ substantially from each other, although both shift in magnitude.

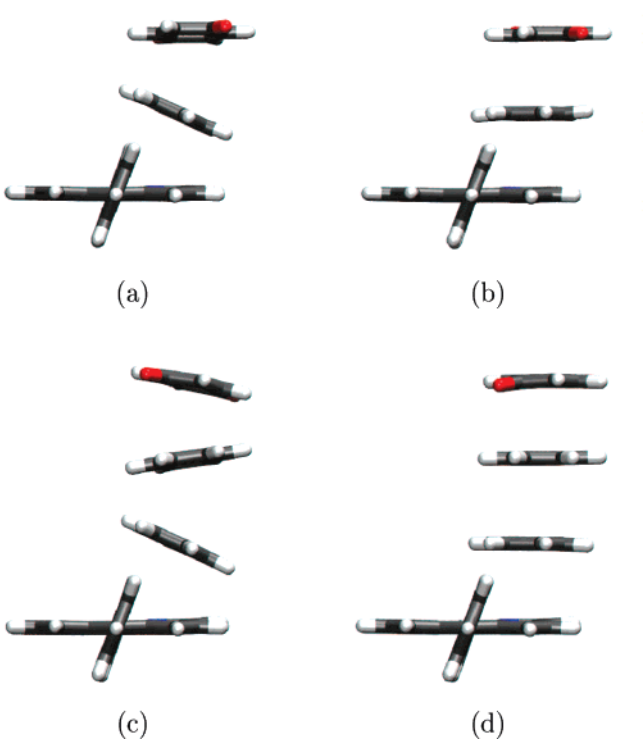

Figure 7. Comparison of partial structures (a) 2a-Zn-4, (b) 2a-Zn-4″, (c) 3a-Zn-9, and (d) 3a-Zn-9″ based on DFT-optimized (2−3)a-Zn geometries. The structures with double prime (b and d) are based on structures (a) and (c) with phenyl and quonyl rings rotated such that they are parallel to the porphyrin plane. Accordingly, the closest atom−atom contacts of (a) and (c) are expanded from 3.0 to 3.5 Å (b and d).

(55) It may seem that the D−A distances for the PM3-based (2−3)a-Zn structures are smaller than those for the DFT-based structures. However, that is because the axis through the centers of the phenyl and quinonyl rings is not perpendicular to the porphyrin plane, not because of tighter stacking of the rings. This can be proven by the fact that the D−A center-to-center distance of PM3-based structures is always about 1 Å larger than that in DFT-based structures.

(56) Tavernier, H. L.; Fayer, M. D. *J. Phys. Chem. B* **2000**, *104*, 11541.
(57) Voityuk, A. A.; Rosch, N.; Bixon, M.; Jortner, J. *J. Phys. Chem. B* **2000**, *104*, 9740.
(58) Tong, G. S. M.; Kurnikov, I. V.; Beratan, D. N. *J. Phys. Chem. B* **2002**, *104*, 2381.
(59) LeBard, D. N.; Lilichenko, M.; Matyushov, D. V.; Berlin, Y. A.; Ratner, M. A. *J. Phys. Chem. B* **2003**, *107*, 14509.
(60) Siriwong, K.; Voityuk, A. A.; Newton, M. D.; Rösch, N. *J. Phys. Chem. B* **2003**, *107*, 2595.
(61) Gupta, S.; Matyushov, D. V. *J. Phys. Chem. A* **2004**, *108*, 2087.
(62) Matyushov, D. V. *J. Chem. Phys.* **2004**, *16*, 7532.
(63) Troisi, A.; Ratner, M. A.; Zimmt, M. B. *J. Am. Chem. Soc.* **2004**, *126*, 2215.
(64) Lewis, F. D.; Liu, J.; Weigel, W.; Rettig, W.; Kurnikov, I. V.; Beratan, D. N. *Proc. Natl. Acad. Sci. U.S.A.* **2002**, *99*, 12536.

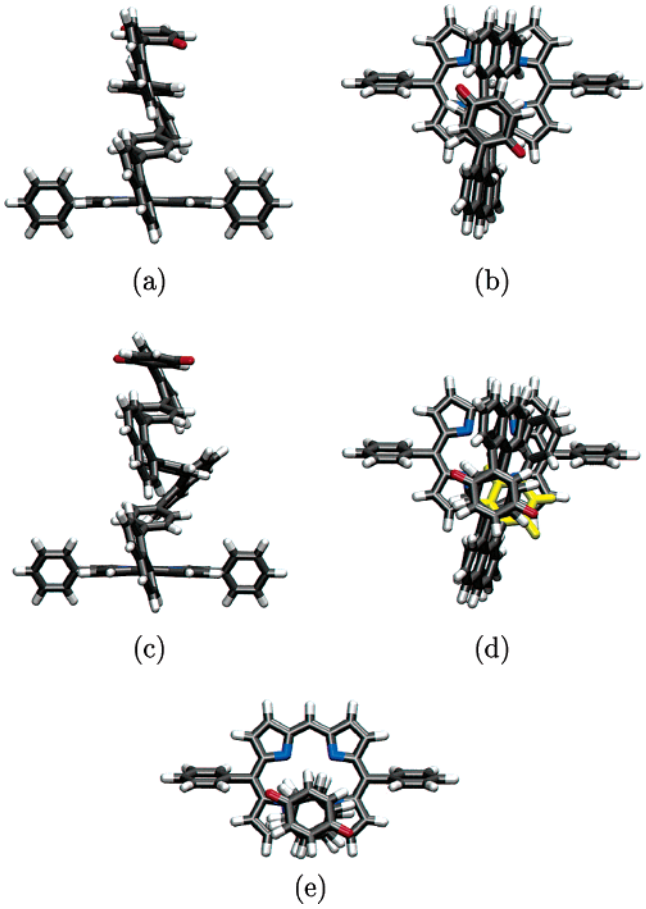

Figure 8. (a) and (b) Side and top views of DFT-based structures 3a-Zn, respectively. (c) and (d) Side and top views of 4a-Zn. The position of the middle phenyl ring of 4a-Zn ((d) highlighted in yellow) shifts significantly compared with the other rings. (e) Top view of modified 4a-Zn′, which is a modified structure of 4a-Zn with all the naphthyl rings removed and the middle phenyl ring moved into the stack.

4. Summary and Conclusions

We have carried out the first comprehensive analysis of electronic coupling interactions in synthetic compressed π-stacked organic systems. The strong dependence of coupling on ring compression makes these systems much more sensitive to geometry change than more familiar linear chain ET systems.

GMH analysis allowed us to interpret the π-mediated electronic couplings in stacked porphyrin−π-bridge−quinone systems. The analysis indicates that this series of structures has a coupling that decays weakly with distance because of the compression of the stack. The phenyl rings provide the crucial tunneling mediation, and the small β value arises from compression of the π-stack. Since the distance dependence of λ_o is expected to be weak (as in other π-stacked ET systems), β^r and β are expected to be nearly the same in these systems. In larger π-stacks (e.g., 4a-Zn), shifting one of the phenyl rings out of register with the other phenyls leads to a predicted large decrease in the ET rate.

We have based both our CS and CR calculations on the ground-state structures. This may account, in part, for the similarity of the coupling in the two processes. More advanced calculations that provide a better description of the electronic structure and geometric relaxation of the excited state are of great interest.

Acknowledgment. D.N.B. thanks the NIH (GM57876) and Duke University for support of this research. M.J.T. thanks DOE (DE-FG02-02ER15299) for its support.

Supporting Information Available: The scheme for building the 3a-Zn DFT structure, proton labeling scheme for 2a, and interplanar distances labeling scheme for 1,8-diphenylnaphthalene and compound **2a**. This material is available free of charge via the Internet at http://pubs.acs.org.

JA050984Y